Draft version May 15, 2017
Preprint typeset using LaTeX style emulateapj v. 12/16/11

AB-INITIO SIMULATIONS OF RADIATIVE MAGNETIC RECONNECTION

Alexander A. Philippov[1,4], Dmitri A. Uzdensky[2,3], Hayk L. Hakobyan[1]

Draft version May 15, 2017

ABSTRACT

We study radiative magnetic reconnection in the environment of coronae of accretion disks around black holes, where the feedback of the inverse Compton drag starts to limit the particle acceleration. Also, the high-energy up-scattered photons are capable to produce secondary electron-positron pairs, which needs to be taken into account. In this draft we present the numerical approach within multi-dimensional PIC simulation that will allow to calculate the particle and radiation spectrum, and also the pair yield in reconnection layers near black holes from first principles. We present the first simulation results, but please acknowledge their very preliminary character.

1. INTRODUCTION

Particle acceleration in relativistic magnetic reconnection has been invoked to explain observed non-thermal radiation in numerous astrophysical sources, e.g., pulsar magnetospheres and wind nebulae (PWN), jets from active galactic nuclei (AGN) and gamma-ray bursts (GRBs) (Hoshino and Lyubarsky 2012). The last decade saw tremendous progress in modeling the plasma energization process using 2D and 3D particle-in-cell (PIC) simulations (Sironi and Spitkovsky 2014; Guo *et al.* 2014; Werner *et al.* 2016a). All these studies found efficient particle acceleration and robust formation of non-thermal power-law tails at high magnetization values. However, in most mentioned astrophysical sources reconnection proceeds in the regime when radiation losses become severe and may well limit the energization process (Uzdensky 2016). The first steps in exploring the radiative regime were done for the case when synchrotron emission is the dominant mechanism of energy losses (Cerutti *et al.* 2013). In this draft we investigate the role of inverse-Compton cooling on particle acceleration and calculate the emission signature. This regime is most relevant for understanding the non-thermal emission from coronae of accretion disks around black holes (Uzdensky 2016; Beloborodov 2017). Moreover, in these environments high-energy photons produced by accelerated particles are capable of electron-positron pair production via the Breit-Wheeler process. For the first time, we add these two important ingredients to kinetic simulations of relativistic magnetic reconnection and show that this approach is capable of predicting the radiative efficiency and the pair yield of accretion disks from first principles.

2. METHODS

2.1. *Physical parameters and simulation setup*

Standard magnetic reconnection problem is defined by three dimensionless numbers: $\sigma_0 = B_0^2/[4\pi n(m_i + m_e)c^2]$, m_i/m_e and L/ρ_σ, where σ_0 is the usual cold magnetization parameter, n, B_0 defines the plasma density and magnetic field strength in the upstream of the reconnecting layer, L is the system size and ρ_σ is the typical Larmor radius of the accelerated particles, $\rho_\sigma = \rho_0\sigma$, $\rho_0 = m_e c^2/eB_0$. The characteristic energy scales for both species are $\sigma_e \approx (m_i/m_e)\sigma_0$ and $\sigma_i \approx \sigma_0$. For simplicity, in this draft we restrict to the case of pair plasma and focus on highly relativistic regime $\sigma_0 \gg 1$. The electron-ion relativistic case, which is most relevant for astrophysical black holes, has recently gained interest (Melzani *et al.* 2014; Werner *et al.* 2016b), and we will investigate it in our future work. Inclusion of the Compton drag and pair production adds the following parameters: U_{rad}, the energy density of soft background photons, which represent the thermal radiation of the accretion disk, and ϵ_{soft}, the mean photon energy. For simplicity, in this draft we consider zero guide field. For simulating relativistic plasma we use massively parallel PIC code TRISTAN-MP (Spitkovsky 2005), significantly modified for simulating the inverse-Compton cooling and photon-photon pair production.

For simplicity, we study relativistic magnetic reconnection in the double-periodic setup with two Harris current layers. The magnetic pressure outside the sheets is balanced by the pressure of hot plasma inside the sheets, which has an overdensity of $\eta = 3$ relative to the cold particles outside the reconnection layers. The pressure equilibrium then sets the plasma temperature inside each sheet to be $T_{sheet} = \sigma/2\eta$ (Sironi and Spitkovsky 2014). We typically initialize our simulations with thin sheets (width of 5 plasma skin depths) and let the reconnection start from the numerical noise. The computational box has the aspect ratio of $L_y/L_x = 2$ and its size is fixed to be $L/\sigma\rho_0 = 140$ in all setups, such that our results are not limited by the small system size (Werner *et al.* 2016a). We run our simulations for 5 light-crossing times of the simulation box. The relativistic skin-depth of the upstream plasma is always resolved with at least 10 cells. We typically use 4 particles per cell to represent the background plasma, however, we tested that our results are unchanged when using up to 32 particles per cell.

2.2. *Numerical algorithm for radiation and pair production*

[1] sashaph@princeton.edu
[2] Center for Integrated Plasma Studies, Physics Department, University of Colorado, Boulder, CO 80309
[3] Institute for Advanced Study, Einstein Drive, Princeton, NJ 08540
[4] sashaph@princeton.edu

Traveling through the bath of soft photons, particles experience an inverse-Compton radiation drag:

$$\mathbf{f}_{drag} = -\frac{4}{3}\sigma_T U_{rad}\gamma^2\frac{\mathbf{v}}{c}. \quad (1)$$

Introducing $\gamma_{rad} = \sqrt{3|e|E/(4\sigma_T U_{rad})}$, which is the radiation-reaction limited Lorentz factor of particles immersed in electric field $E = \beta_{rec}B$, $\beta_{rec} \approx 0.1$ is the fiducial reconnection rate value, we can write the expression for the drag force as

$$\mathbf{f}_{drag} = -|e|\beta_{rec}B_0\left(\frac{\gamma}{\gamma_{rad}}\right)^2\frac{\mathbf{v}}{c} \quad (2)$$

In order to take pair production into account, we represent Compton upscattered photons as a separated specie of simulation particles. In the simulation domain we only track photons with energies $\epsilon > (m_e c^2)^2/\epsilon_{max}$, which will contribute to pair production, and ϵ_{max} is the expected maximum energy of upscattered photons. The corresponding maximum Lorentz factor of accelerated electrons is $\gamma_{max} = \sqrt{\epsilon_{max}/\epsilon_{soft}} \approx \min(\gamma_{rad}, \gamma_{c1}, \gamma_{c2})$, where γ_{rad}, $\gamma_{c1} = 4\sigma$ and $\gamma_{c2} = \beta_{rec}L/\rho_0$ represent the particle energy limits due to radiation losses, magnetization and the system size in the double-periodic problem as found by Werner *et al.* (2016a). The pair producing photons are produced in upscattering of soft photons by particles with Lorentz factors $\gamma > \gamma_{min} = \gamma_c(\gamma_c/\gamma_{max})$, where $\gamma_c = \sqrt{m_e c^2/\epsilon_{soft}}$ corresponds to energy of particle, which is capable to produce the photon of energy $m_e c^2$. In order to avoid the double counting, we treat radiation drag for particles with energy $\gamma < \gamma_{min}$ as a continuous force, while drag on particles, which emit pair-producing photons, is applied only when the photon is radiated.

The numerical algorithm should take into account production of photons, their propagation, collisions with other photons, pair creation. These are the steps we describe below.

Production of photons. If a particle reaches an energy $\gamma > \gamma_{min}$, it can create a photon of energy $\epsilon_{soft}\gamma^2 = m_e c^2(\gamma/\gamma_c)^2$ which is created with a probability per time step Δt

$$\tau_{IC} = \frac{4}{3}n_{soft}\sigma_T v\Delta t = \frac{4}{3}\frac{U_{rad}}{\epsilon_{soft}}\sigma_T v\Delta t, \quad (3)$$

where $v\Delta t \approx c\Delta t$ is the distance that a particle travels per one computational timestep. We express $U_{rad} = (3e\beta_{rec}B_0)/(4\sigma_T\gamma_{rad}^2)$ and $\epsilon_{soft} = m_e c^2/\gamma_c^2$ through γ_{rad} and γ_c using definitions given above and obtain

$$\tau_{IC} = \beta_{rec}\left(\frac{\gamma_c}{\gamma_{rad}}\right)^2\left(\frac{v\Delta t}{\rho_0}\right). \quad (4)$$

This equation involves only the ratio γ_c/γ_{rad} as a parameter. If a photon is created, we subtract the momentum of the freshly created photon $\mathbf{p}_{ph} = m_e c(\gamma/\gamma_c)^2\mathbf{n}$ from parent particle momentum, where $\mathbf{n}$ is the unit vector along the particle direction of motion. The average energy and momentum loss rate in this process coincides with one given by the continuous description of the radiation drag. For example, the average momentum loss per unit time (the radiation drag force) is

$$-\frac{\tau_{IC}\mathbf{p}_{ph}}{\Delta t} = -\frac{4}{3}\frac{U_{rad}}{\epsilon_{soft}}\sigma_T v\frac{\epsilon_{soft}}{c}\gamma^2\mathbf{n} = \mathbf{f}_{drag}. \quad (5)$$

This description is valid as long as the energy of the produced photon, $\epsilon_{soft}\gamma^2 = m_e c^2(\gamma/\gamma_c)^2$, is much smaller than the electron energy $m_e c^2\gamma$. This results in the condition $\gamma \ll \gamma_c^2$. Given that we expect $\gamma_{max} \approx \gamma_{rad}$ for sufficiently large system sizes, this is equivalent to $\gamma_{rad} \ll \gamma_c^2$. This implies the minimum energy of electrons, which emit potentially pair-producing photons $\gamma_{min} = \gamma_c^2/\gamma_{rad} \gg 1$, so everything is self-consistent.

Propagation of photons. Simulation photons travel at the speed of light and propagate along straight lines. Boundary conditions for the photons and other simulation particles are the same, e.g., periodic or outflow.

Photon collisions and pair creation. For a pair of photons with energies ϵ_1 and ϵ_2, pair creation is possible if $s = \epsilon_1\epsilon_2(1-\cos\alpha)/2(m_e c^2)^2 > 1$. Here, s is a relativistic invariant and defines the energy of the colliding photons in the center of mass frame (CMS), $2\sqrt{s}m_e c^2$, and α is the angle between the two photons. The total cross section for pair production, which is a relativistic invariant, can be found using standard Breit-Wheeler formula (Berestetskii *et al.* 1971). The cross-section behaves as $\sqrt{s-1}$ near $s \approx 1$, has a peak around $s \approx 2$ and decreases as $1/s$ for higher CMS energy.

The pair production calculation represents a loop over simulation photons of the energy ϵ_1.

- Create a list of photons ordered by energy in a given collision volume V_{coll} (could be one cell or more, depending on the quality of the photon statistics), with energies capable of pair production: $2(m_e c^2)^2/[(1-\cos\alpha)\epsilon_1] < \epsilon_2 < \epsilon_1$. Compute its length N_{ph}.

- Compute probabilities of $\gamma-\gamma$ binary interactions per timestep:

$$\tau_i = \sigma_i(\epsilon_1, \epsilon_2, \alpha)c\Delta t/V_{coll}. \quad (6)$$

  The total probability for the photon to decay at this timestep is:

$$\tau = \sum_{i=1}^{N_{ph}}\tau_i = \tau_0\frac{\sum_{i=1}^{N_{ph}}\left(\frac{\sigma_i}{\sigma_T}\right)}{n_\gamma}\frac{c\Delta t}{L}, \quad (7)$$

  where i is the summation index over the photon list. Here

$$\tau_0 = n_{soft}\sigma_T L \quad (8)$$

  is the fiducial optical depth, which can be expressed through other radiative parameters as $\tau_0 = 3/4(L/\rho_0)(\gamma_c/\gamma_{rad})^2$. This probability defines whether a photon will pair-produce at a given timestep. If not, the loop goes to the next photon.

- If a photon is decided to pair produce, we define normalized probabilities of interaction with each photon in the cell $\tilde{\tau}_i = \tau_i/\tau$, an array $X_i = X_{i-1} + \tilde{\tau}_i, X_0 = 0, 1 < i < N_{ph}$, and a random number $0 < \xi < 1$. Photon ϵ_1 interacts with a photon of index i in the array if $X_{i-1} < \xi < X_i$.

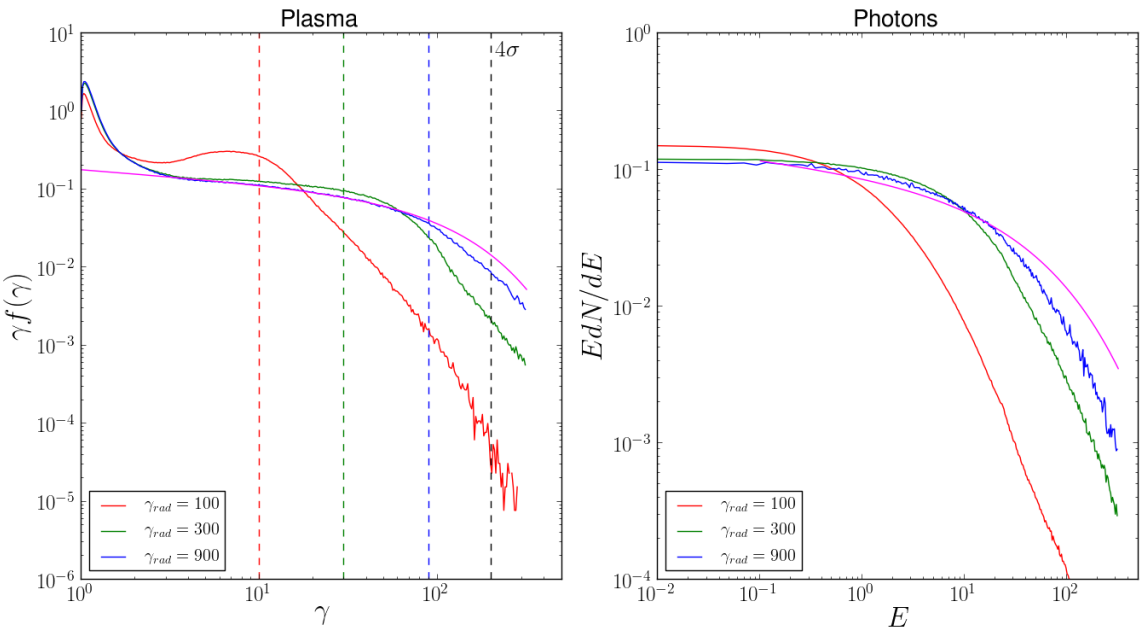

FIG. 1.— Simulation of the relativistic magnetic reconnection of $\sigma = 50$ with inverse-Compton cooling being included but without pair production. Left panel: Particle spectrum. Right panel: Radiation spectrum. All energies are normalized to $m_e c^2$. On both plots the solid magenta curve shows the fit of the uncooled simulation by Werner *et al.* (2016a). The colored dashed vertical lines shows the $\gamma_{rad}/10$ energy, and the black dashed vertical line is at $\gamma_{c1} = 4\sigma$.

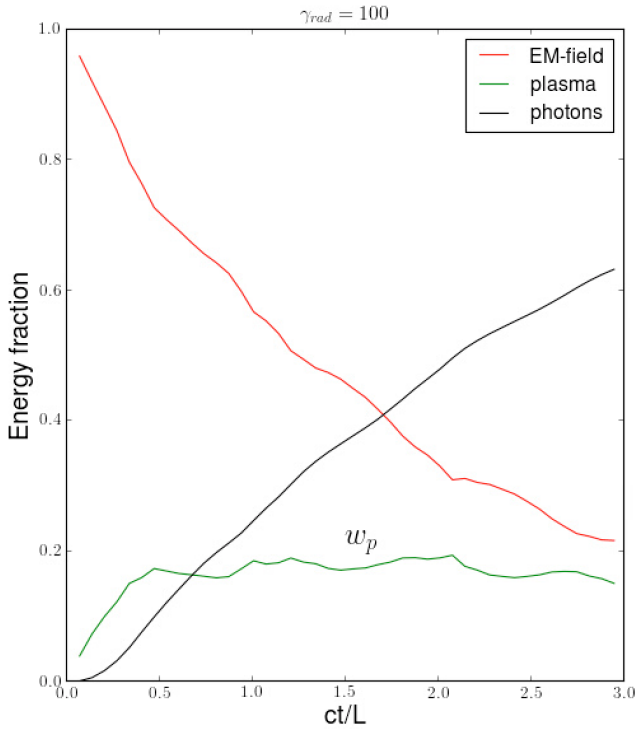

FIG. 2.— Energy partition in the simulation $\sigma = 50$, $\gamma_{rad} = 100$ as a function of simulation time.

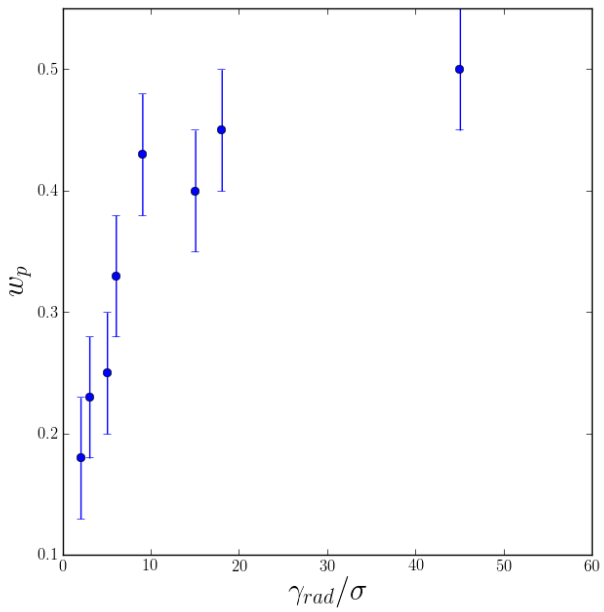

FIG. 3.— The fraction of energy in plasma as a function of the ratio of simulation parameters, γ_{rad} and σ.

- Kinematics of the binary interaction. We consider the process in the CMS frame. The 3-velocity of this frame is

$$\mathbf{V_{CMS}} = c^2 \frac{\mathbf{P_1} + \mathbf{P_i}}{\epsilon_1 + \epsilon_i}. \quad (9)$$

In this frame, the produced electron and positron have equal energies $\epsilon_+ = \epsilon_- = \sqrt{s}$ and oppositely directed momenta $\mathbf{p}_- = -\mathbf{p}_+$. The probability distribution of the angle θ between the momentum of the produced particle and mometum of the photon $\mathbf{P_1}$ is given by the differential cross-section $\mathrm{d}\sigma/\mathrm{d}\theta$. Second angle, ϕ, which is in the plane perpendicular to $\mathbf{P_1}$, is a uniformly distributed random number. Once the two angles ϕ and θ are defined, the

particle momenta in the CMS frame is fully determined. The momenta in the simulation frame are obtained by the Lorentz transformation with the velocity $-\mathbf{V_{CMS}}$.

To summarize, the simulation is described by three additional dimensionless numbers, compared to the ordinary reconnection problem: γ_c, γ_{rad}. By varying these numbers, we will study different regimes of the reconnection with pair production. For the black-body spectra of soft photons from the disk, one can find:

$$\gamma_c = 6\left(\frac{\theta_e}{10^{-2}}\right)^{-1/2}, \tag{10}$$

$$\frac{\gamma_{rad}}{\gamma_c} \approx 25\left(\frac{B}{10^6\mathrm{Gs}}\right)^{1/2}\left(\frac{\theta}{10^{-2}}\right)^{-2}, \tag{11}$$

where θ_e is the disk temperature in units of $m_e c^2$ and B_d is the disk's magnetic field. While exploring the full parameter space is a very ambitious project, in this draft we present the first steps on this path.

3. RESULTS

In our simulations magnetic reconnection starts from the numerical noise. As a result of the tearing instability, the reconnection layer breaks into a series of magnetic islands, separated by X-points. Over time, the islands coalesce and grow to larger scales. Secondary current sheets produced in the evolution become unstable to the plasmoid instability, which produces the hierarchical structure of X-points and plasmoids (e.g., Uzdensky *et al.* 2010). This picture is unchanged when inverse-Compton cooling and pair production are added to simulations. Interestingly, the value of the reconnection rate is also insensitive to cooling and stays at $\approx 0.15c$ in all our simulations. In next subsections, we discuss how cooling and pair production affect particle acceleration and radiation spectrum.

3.1. *IC cooling*

First, we run simulations with IC cooling but without the pair production. For each value of the magnetization parameter $\sigma = 20, 50, 100$ we investigate several values of $\gamma_{rad} = 100, 300, 900$. As γ_{rad} decreases and becomes comparable to $\approx 10\sigma$, we find that inclusion of the inverse-Compton cooling significantly limits the particle acceleration. Unlike synchrotron losses studied previously (Cerutti *et al.* 2013), inverse-Compton losses do not decrease inside the reconnection layer and dramatically increase as the particle reaches energies of order of γ_{rad}. In Figure 1 we show the particle and radiation spectra for $\sigma = 50$ and the range of γ_{rad} values, which we find to be generic for all magnetization values we simulated. The solid magenta line in the plot of the particle spectrum corresponds to the fit of the uncooled simulation by Werner *et al.* (2016a), $\approx \gamma^{-p}\exp(-\gamma/4\sigma)$, where $p \approx 1.2$. As is clearly seen, only simulation with $\gamma_{rad} = 900$ shows similar spectrum. As γ_{rad} decreases, a strong bump at energies $\gamma \approx \gamma_{rad}/10$ starts to develop. These particles are radiation-reaction limited and can not accelerate to significantly higher energies. As more and more particles gain energy in the reconnection process and accumulate at the bump, the spectrum at $\gamma < \gamma_{rad}/10$ also gets modified, so that the effective power-law index of the spectrum at these energies increases. There is a hard cut-off of the spectrum at energies higher than $\approx \gamma_{rad}/10$, where the particle spectrum can be fitted as a steep power-law γ^{-5}.

The IC radiation spectrum is shown in the right panel of Figure 1. Here, the solid magenta line shows the spectrum of inverse-Compton photons, which corresponds to the fit of the uncooled particle spectrum. The photon power law index Γ, which is defined as $dN/dE \propto E^{-\Gamma}$, is connected with the particle power law index p as $\Gamma = (p+1)/2$. As $p \to 1$ for high magnetization values, the radiation spectrum asymptotes to $\Gamma \approx 1$. The cut-off of the particle spectrum is naturally imprinted on the photon spectrum. As γ_{rad} decreases, the density of high-energy photons decreases, and most of the radiation power is radiated at below-MeV energies.

We also investigate the energy partition between the magnetic field, photons and plasma. The typical energy evolution in the simulation is shown in Figure 2. At low values of γ_{rad} (which correspond to high radiation energy density U_{rad}), most of the dissipated magnetic energy goes into radiation, while energy of the plasma stays at the radiation-reaction limited value, which is referred to as w_p. At the end of the plasmoid-dominated stage of reconnection, the fraction $\approx (0.5 - w_p)$ of the initial magnetic field energy is released into photons. Obviously, this fraction increases as γ_{rad} decreases. The calculated dependence of w_p on simulation parameters is reported in Figure 3. Interestingly, even when the most active reconnection event is over at $t \approx 1.5L/c$, the magnetic energy keeps decreasing for low values of γ_{rad}, which are comparable to σ. At this stage, the simulations box have two large plasmoids, which consist of the hot plasma that keeps emitting inverse-Compton photons. As the pressure support ceases, the plasmoid gradually shrinks and more magnetic field energy is dissipated into plasma energy, which is immediately radiated away in the form of photons.

3.2. *Pair production*

In this section we report the results of simulations with pair formation included. We focused on the following set of parameters: $\sigma = 50, \gamma_{rad} = 300$ and a range of values of $\gamma_c = 10, 30, 40$.

In Figure 4 we show a simulation snapshot, which represents the density distribution of all simulation species. We find that most of the pairs are produced in plasmoids, where counter-streaming beams of high-energy photons from neighbouring X-points collide. Pairs are later injected into the acceleration process in colliding islands, etc. - to be investigated in the future work. In Figure 5 we show the plasma and photon spectra in the simulation. The difference in the acceleration history of the initial plasma particles and produced pairs is clearly imprinted in the energy spectra. We argue that secondary pairs did not go through the primary X-point, and that is why their spectra is significantly softer and does not follow the spectra of primary particles. As for the energy partition, we find that our pair producing simulation at $\gamma_c = 20$ reached rough equipartition between the initial plasma and produced pairs. In the explored parameter range, the multiplicity of secondary pairs is

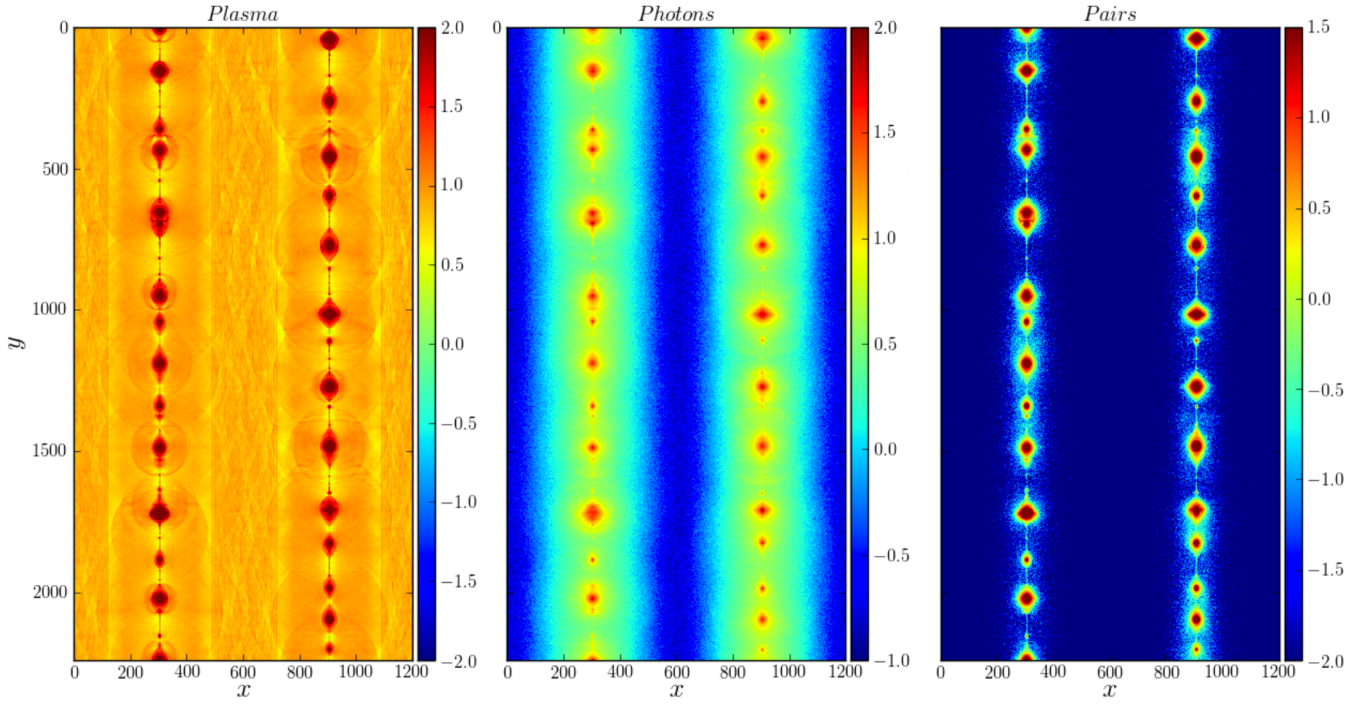

FIG. 4.— Density of simulation species in the pair producing simulations at $\sigma = 50$ and $\gamma_{rad} = 300$.

mainly determined by the increase of τ_0 and decrease of the high-energy photon number density at high γ_c. The two effects nearly cancel each other, and we find slight increase of the plasma multiplicity at higher γ_c. As a reference, at the end of the active reconnection event at $t \approx 1.5L/c$ our simulation at $\gamma_c = 40$ produces as much plasma charges as it was initially in the simulation box. Availability of performing such simulations opens the possibility to explore the regime when produced pairs will produce significant feedback on the reconnection dynamics, as is expected to happen near astrophysical black holes (Beloborodov 2017).

4. CONCLUSIONS

We outlined the kinetic method of simulating radiative reconnection with pair production. In this draft we applied it to exploring the inverse-Compton cooling dominated current layers, which likely occur in the coronae of accretion disks around black holes. We found the reconnection rate remained unchanged by the cooling losses in all our simulations, and the micro-physical interpretation of this conclusion will be clarified in our future work. When radiation losses became severe at low γ_{rad}, we found that particle acceleration ceased at energy $\approx \gamma_{rad}/10$, and characteristic bump in the particle spectrum was created. As γ_{rad}/σ decreased, systematically higher fraction of the initial magnetic energy was radiated away of the reconnection layer, at progressively lower energies. We also performed first steps in exploring the parameter space taking into account pair production. We found that most of secondary pairs are produced in plasmoids. The difference in acceleration history of initial plasma particles and secondary pairs produced a difference in their spectra.

In the future work we plan to perform simulations of the synchrotron-cooled reconnection sheets. This should allow to self-consistently calculate the pair yield of current sheets of young pulsars with the high magnetic field at the light cylinder (Lyubarskii 1996), where the Breit-Wheeler process may well be the dominant channel of charge production.

5. ACKNOWLEDGEMENTS

This research was supported by Porter Ogden Jacobus Fellowship awarded by Princeton University to A. A. Philippov and was facilitated by Max Planck/Princeton Center for Plasma Physics. D. A. Uzdensky gratefully acknowledges the hospitality of the Institute for Advanced Study and support from the Ambrose Monell Foundation. This work was also supported by DOE grant DE-SC0008409, NASA grant NNX16AB28G, and NSF grant AST-1411879. The simulations presented in this article used computational resources supported by the PICSciE-OIT High Performance Computing Center and Visualization Laboratory.

REFERENCES

M. Hoshino and Y. Lyubarsky, Space Sci. Rev. **173**, 521 (2012).
L. Sironi and A. Spitkovsky, ApJ **783**, L21 (2014), arXiv:1401.5471 [astro-ph.HE].
F. Guo, H. Li, W. Daughton, and Y.-H. Liu, Physical Review Letters **113**, 155005 (2014), arXiv:1405.4040 [astro-ph.HE].
G. R. Werner, D. A. Uzdensky, B. Cerutti, K. Nalewajko, and M. C. Begelman, ApJ **816**, L8 (2016a), arXiv:1409.8262 [astro-ph.HE].
D. A. Uzdensky, Magnetic Reconnection: Concepts and Applications **427**, 473 (2016), arXiv:1510.05397 [astro-ph.HE].
B. Cerutti, G. R. Werner, D. A. Uzdensky, and M. C. Begelman, ApJ **770**, 147 (2013), arXiv:1302.6247 [astro-ph.HE].

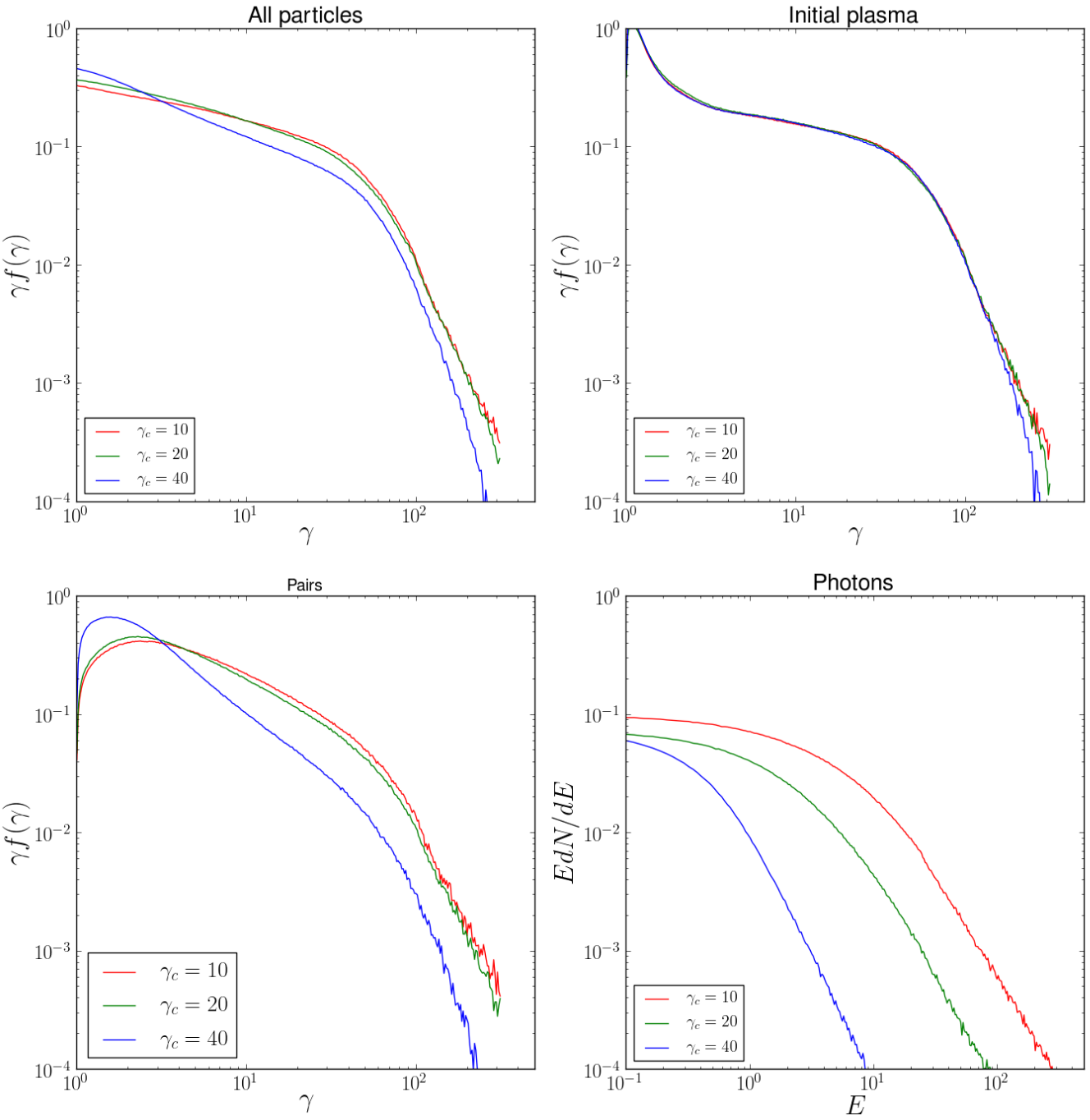

FIG. 5.— Spectrum of different simulation species in the pair producing simulations at $\sigma = 50$ and $\gamma_{rad} = 300$. All energies are normalized to $m_e c^2$.

A. M. Beloborodov, ArXiv e-prints (2017), arXiv:1701.02847 [astro-ph.HE].

M. Melzani, R. Walder, D. Folini, C. Winisdoerffer, and J. M. Favre, A&A **570**, A112 (2014), arXiv:1405.2938 [astro-ph.HE].

G. R. Werner, D. A. Uzdensky, M. C. Begelman, B. Cerutti, and K. Nalewajko, ArXiv e-prints (2016b), arXiv:1612.04493 [astro-ph.HE].

A. Spitkovsky, in *Astrophysical Sources of High Energy Particles and Radiation*, AIP Conf. Ser., Vol. 801, edited by T. Bulik, B. Rudak, and G. Madejski (2005) p. 345.

V. B. Berestetskii, E. M. Lifshitz, and V. B. Pitaevskii, *Course of theoretical physics - Pergamon International Library of Science, Technology, Engineering Social Studies, Oxford: Pergamon Press, 1971, edited by Landau, Lev Davidovich (series); Lifshitz, E.M. (series)* (1971).

D. A. Uzdensky, N. F. Loureiro, and A. A. Schekochihin, Physical Review Letters **105**, 235002 (2010), arXiv:1008.3330 [astro-ph.SR].

Y. E. Lyubarskii, A&A **311**, 172 (1996)